Ectomycorrhizal utilization of different phosphorus sources in a glacier forefront in the Italian Alps

Ectomycorrhizal utilization of different phosphorus sources in a glacier forefront in the Italian Alps

Michele D'Amico[1*], Juan Pablo Almeida[2], Sonia Barbieri[1], Fabio Castelli[1], Elena Sgura[1], Giulia Sineo[1], Maria Martin[1], Eleonora Bonifacio[1], Håkan Wallander[2], Luisella Celi[1]

[1]*DISAFA, Università degli Studi di Torino, Largo Braccini 2, Grugliasco (TO), Italy.*
[2]*Department of Biology, MEMEG, Lund University, Sölvegatan 37, 223 62 Lund, Sweden*
*corresponding author: ecomike77@gmail.com; +393490611313

ABSTRACT

Aims

In deglaciated surfaces, lithology influences habitat development. In particular, serpentinite inhibits soil evolution and plant colonization because of insufficient phosphorus (P) content, among other stressful properties. In nutrient-poor environments, ectomycorrhizal fungi (EMF) play a key role exploring the soil for P beyond the rhizosphere. In this study, we followed the role of EMF in accessing inorganic and organic P along two proglacial soil chronosequences in the Alps (NW Italy), respectively characterized by pure serpentinite till and serpentinite mixed with 10% of gneiss, and colonized by European Larch.

Methods

The access to inorganic and organic P forms by EMF was studied using specific mesh-bags for fungal hyphae entry, filled with quartz sand and inorganic phosphate (Pi) or myo-inositolhexaphosphate (InsP6) adsorbed onto goethite. They were incubated over 13 months at the organic/mineral horizon interface. After harvesting, EMF colonization via ergosterol analysis and the amount of P and Fe removed from mesh bags were measured.

Results

Ergosterol increased along the two chronosequences with slightly greater values on serpentinite and in Pi-containing bags. Up to 65% of Pi was removed from mesh-bags, only partly accompanied by a parallel release of Fe. The amount of InsP6 released was instead less than 45% and mostly removed with goethite.

Conclusions

The results suggest that, in extremely P-poor environments, EMF are able to release both inorganic and organic P forms from highly stabilized associations.

Keywords

Ectomycorrhizae; Mesh bags experiment; Phosphorus uptake; Primary succession; Serpentinite soils; Soil chronosequence

Abbreviations

ectomycorrhizal fungi: EMF; *myo*inositol hexaphosphate: InsP6; serpentinite sites: S sites; serpentinite sites with 10% gneiss: SG sites

Introduction

Glacier retreat induced by climate change in Alpine habitats, occurring with few interruptions since the end of the Little Ice Age around 1860, creates habitats characterized by different ages, which coexist over short distances (Burga et al. 2010). Within this environment, igneous, metamorphic or sedimentary rocks can be exposed, leading to the development of soils differing in chemical and physical characteristics (Rajakaruna and Boyd 2008). Thus, lithology is the first factor that drives soil formation and controls its evolution. In particular, serpentinite slows down pedogenic processes because of various limiting factors for plant colonization. In fact, serpentinite soils are characterized by low calcium to magnesium (Ca/Mg) ratios and frequently contain high levels of heavy metals, which are toxic to most plants. In addition, these soils are often very poor in nutrients, especially phosphorus (Brooks 1987).

Many plant species have evolved in P-poor environments and, as a consequence, are known to possess a number of adaptive features to respond to P starvation by increasing the ability of their root systems to acquire P from the soil (White et al. 2005; Hammond and White 2008; Lynch and Brown 2008; White and Hammond 2008; Fang et al. 2009). For instance, many plants, such as *Larix decidua* Mill. in the European Alps, form symbiotic relationships with ectomycorrhizal fungi (EMF) to increase their ability to explore the soil volume and mobilize nutrients from remote inorganic and organic sources (Bucher 2007; Smith and Read 2008; Jansa et al. 2011). Basically, the host plant receives mineral nutrients via the fungal mycelium, while the symbiotic fungus

obtains carbon photosynthetates from the host plant (Harley and Smith 1983). The benefits these symbiotic associations impart to plants include enhanced enzyme activity (Read and Perez-Moreno 2003; Plassard et al 2011; Cairney 2011), production of secondary metabolites (Shah et al 2015) and improved water uptake under drought stress (Courty et al 2010), which can further enhance P uptake and its availability for the host plant. It has been indeed reported that EMF growth in P-limited soils is enhanced due to a higher carbon investment from the plant to the fugal symbionts to enhance P foraging (Rosenstock et al. 2016; Almeida 2019). These strategies should overcome the constraints due to the low P content or to the low availability of P in soils with high retention capacity.

In general, P retention, involving both adsorption and/or surface precipitation, is related to the different affinity of inorganic and organic P compounds for iron (Fe) and aluminium (Al) (hydr)oxides (Celi et al. 1999, 2001, 2003; Yan et al. 2014). Because of their high affinity, inositol phosphates undergo a selective enrichment in the soil with respect to other organic and inorganic P forms (Darch et al. 2014; George et al. 2018; Magid et al. 1996). Interaction of inositol phosphates with mineral phases has been reported to limit enzymatic hydrolysis and hamper their biodegradation in both controlled (Giaveno et al., 2010) and natural systems (George et al. 2007).

The presence of EMF significantly modifies soil conditions in the rooting zone by producing various compounds that can favour the release of P from the adsorbed surfaces (Landerweert et al 2001; Richardson et al. 2011).

This may occur through three main mechanisms: i) competition of organic acid anions by ligand exchange for the same adsorption sites (Rosling 2009); ii) dissolution of minerals by organic acids via ligand exchange and metal complexation; and iii) reductive iron oxide dissolution by electron donor compounds such as polyphenolic compounds (Shah et al. 2015). These mechanisms have been studied mainly for P desorption from mineral surfaces. Several forms of organic P are accessible to EMF through excretion of phosphatases (Cairney 2011, Louche et al 2010, Smith et al 2018), but to what extent these P sources is available to EMF when they are adsorbed on mineral surfaces have never been explored.

Thus, the aim of this study is to evaluate the role of mycorrhizal fungi in accessing P adsorbed on goethite in two soil chronosequences characterized by different levels of P limitation in the proglacial area of Verra Grande Glacier (Aosta Valley, Italy). Both chronosequences are characterized by serpentinitic parent materials. In previous works (D'Amico et al. 2015, 2017) we observed a slow soil evolution and plant primary succession due to serpentinite lithology. Small quantities of gneiss in one of the chronosequences can partly compensate the harsh conditions for biota and enhance plant colonization and pedogenesis.

In these environments we hypothesized that: i) soil P forms and cycling were strongly affected by the little differences of the parent material; ii) EMF development was more expressed in the most-limited soils; iii) EMF were able to access different P sources. In order to test these hypotheses i) we evaluated soil P dynamics along the two chronosequences, and ii) we followed the development of EMF and iii) their capacity to access P by using mesh bags filled with inorganic and organic P forms retained by a Fe oxide-sand system and incubated in the two soil chronosequences for thirteen months.

Materials and methods

Study area

The study area is located in the upper Ayas Valley (Aosta Valley, north-western Italian Alps), in the Verra Grande Glacier forefield (Fig. 1). There is not a precise dating of the Verra Grande moraine system. However, the presence of morainic arches not affected by the erosive action of the Evançon creek allowed an approximate deposition dating, based on similarities with nearby and better studied glacier forefields (e.g. D'Amico et al. 2015).

The study area is characterized by two different lithologies: pure serpentinite in the western part (S chronosequence) and serpentinite enriched with a small amount of gneiss (10%) in the eastern one (SG chronosequence). This difference in the parent material composition, although small, brought to a different soil evolution and plant primary succession. The S chronosequence is characterized by an extremely slow pedogenesis with low acidification rates, organic matter (SOM) accumulation and mineral weathering. These characteristics make it difficult for plants to colonize the substrate, forming sparse stands even 190 years after the deposition of the moraine. In the SG chronosequence, small amounts of gneiss in the parent material led to an increase in plant colonization rate, together with higher SOM content, mineral weathering and nutrient biocycling (D'Amico et al., 2015).

The climate of the Ayas Valley is continental, typical of inner-alpine zones, characterized by a quite low mean annual precipitation (around 730 mm yr^{-1}, including snow-water equivalent) homogeneously distributed throughout the year. The mean annual temperature is between 0 °C and +2 °C (Mercalli, 2003).

The vegetation growing in the proglacial area is rich in pioneer species dominated by *Salix* ssp. and *Dryas octopetala* L., with a large number of serpentine endemic and Ni-hyperaccumulator species (Vergnano Gambi and Gabrielli, 1981; Vergnano Gambi et al., 1987). Large bare soil areas

characterized the western lateral moraines, and well-developed grasslands on the eastern ones. Scattered portions of the oldest moraines are colonized by *Larix decidua* Mill. forests, while a few Ericaceae (*Rhododendron ferrugineum* L. and Vaccinium ssp.) and *Juniperus nana* Willd. are widely scattered in the understory. A full ericaceous cover is reached in Late Glacial moraines, not considered in this study.

Most of the soils in the proglacial area have been classified as Eutric Skeletic Regosols (IUSS Working Group WRB, 2015). In the oldest moraine area, poorly developed podzols (Entic Podzols) have also been observed, while outside the proglacial area soils were well-developed podzols (Haplic Podzols) on the eastern side of the valley, and Dystric Cambisols on the opposite western slope (D'Amico et al. 2015).

Site selection, soil sampling and analysis

Soil development and the role of mycorrhizae in accessing P along the two chronosequences were investigated by selecting three sites within moraines deposited ca. 70, 190 and 3000 years ago (identified as S70, S190 and S3000 respectively) in the S chronosequence and coeval sites in the SG chronosequence (SG70, SG190 and SG3000). The two series of sites were compared to an area closer to the glacier only recently stabilized after intense paraglacial activity and without vegetation cover, namely S5 and SG5 (Fig. 1). Beyond soil age and parent material, other factors, such as slope steepness, aspect and tree cover were alike.

At each site, five larch trees were selected (except in S5 and SG5, where trees were not present) to cover spatial heterogeneity and soils collected in June 2016, sampling the organic and the first mineral horizons. Each replicate was in turn obtained by three subsamples collected around the tree and pooled together. The samples were air dried and sieved at 2 mm.

Soil pH was measured potentiometrically on a soil/water suspension (soil/water ratio 1:2.5 and 1:20 for mineral and organic samples, respectively). Total C and N were determined by elemental analysis (CE Instruments, NA2100 Protein, Milan, Italy). Carbonates were not present in any samples. Cation exchange capacity (CEC) was determined by the method described by Sumner et al. (1996) and the exchangeable cations (K^+, Ca^{2+}, Mg^{2+} and Ni^{2+}) were measured by atomic absorption spectrometry (AAS, Perkin Elmer 3030, Waltham, Massachusetts, USA). The determination of pseudo-total elements (Fe, Mg, Ni, Cr and Co) was carried out by acid digestion with *aqua regia* (65% HNO_3 and 37% HCl, 1:3) and AAS.

Soil total P content was determined by acid digestion with concentrated H_2SO_4 and $HClO_4$, followed by colorimetric analysis with malachite green (Ohno and Zibiliske, 1991; Martin et al., 1999). Soil available P content was determined using the Olsen method (1954).

Mesh bags preparation and incubation

Production and capacity of EMF to access P forms were determined by incubating rectangular nylon mesh bags (5x9 cm; 50 µm mesh size; Sintab product AB, Malmö, Sweden), allowing fungal hyphae but not roots to penetrate inside, as described by Wallander et al. (2001). Mesh bags were sealed with a manual impulse heat sealer and filled with 15 g of different P-goethite–sand systems prepared as follows. 10.8 kg of quartz sand was used as the main substrate of the bags. The sand was previously sieved at 70 µm and washed with 1M HCl and then with deionized water to remove any P trace and to adjust the pH at 6, respectively. The sand was then dried.

Pure goethite was synthesized as described by Schwertmann and Cornell (1964) using 100 ml of $Fe(NO_3)_3$ and 180 ml of 5M NaOH. Then, 2 l of deionized water was added and the suspension heated at 70 °C for 60 hours. The precipitate was centrifuged, washed and dried. 108 g of goethite were produced and divided into three aliquots. Two aliquots were treated with KH_2PO_4 (Pi-Gt) or *myo*inositol hexaphosphate (InsP6) (InsP6-Gt) respectively, whereas the third one was kept as such (Gt) as control for measuring potential input/output of external elements. To allow a 75% saturation of the goethite surface, 367 mg of KH_2PO_4 and 445 mg of InsP6 were added to 36 g of goethite, respectively. The systems were allowed to react for 24 h, washed with deionized water to remove possible P that did not react with Gt and then each treated Gt system was mixed with 3600 g of the acid-washed sand. The obtained three systems were thereafter named *Gt–sand*; *Pi-Gt–sand*; *InsP6-Gt–sand*; 15g of each system was placed in a mesh bag, thus obtaining 360 mesh bags.

In each site, the three systems were positioned around the five selected trees, except in S5 and SG5, where the mesh bags were placed in the barren area. For each system, three mesh bags were located as subreplicates. In summary, five replicates of each of the three treatments were placed around each tree, and five trees were selected at each of the four age-sites along the chronosequences (3x3x5x4x2). The bags were installed horizontally at the interface between the organic horizon and the mineral soil, as in this portion of soil most of the microbial activity takes place. In S5 and SG5, the bags were installed below the first 2 cm of unweathered till material.

They were incubated in June 2016 and harvested after 13 months. After collection, the 360 mesh bags were stored at 4°C until analysis. The three subreplicates were pooled together and divided into two aliquots: one was stored as such for ergosterol analysis, while the second portion was dried for P and Fe analyses.

Ergosterol determination.

In order to quantify the fungal biomass in the pooled samples, ergosterol was used as biological marker and quantified following the method described by Berner et al. (2012). Ergosterol was extracted using 10% KOH in methanol, separated with cyclohexane and quantified by high-performance liquid chromatography (HPLC) (L2400, Hitachi, Japan). Methanol was used as the mobile phase and quantification was determined by UV detection at 282 nm.

Phosphorus and iron determination.

Total P that remained in the *Gt–sand* and *Pi-Gt–sand* mesh bags after incubation for 13 months (t_{13m}) was determined by acid digestion with HCl whereas total P in the *InsP6-Gt–sand* systems was carried out by treating the samples with concentrated H_2SO_4 and $HClO_4$. Phosphorus determination was performed by following Ohno and Zibilske method (1991). Iron content was determined on the previously dissolved or digested samples by AAS. Total P and Fe determination was performed also on *Gt–sand*, *Pi-Gt–sand* and *InsP6-Gt–sand* systems before incubation (t_0). The difference between the P and Fe findings measured at t_0 and t_{13m} was calculated. The negative values obtained in the *Gt-sand* sets were considered as a gross input of P (P_{input}), whereas the positive values were considered as a gross output from the mesh bags. Net P release was then calculated as follows:

$$net\ P\ release = -(P_0 - P_t)_{Gt} + (P_0 - P_t)_{P-Gt} \quad \text{(Eq.1)}$$

where P_0 is P concentration before incubation, P_t is P concentration after the 13 months incubation in the soil, Gt is the *Gt-sand* system, P-Gt is the *Pi-Gt-sand* system, $(P_0 - P_t)_{Gt}$ refers to the amount of P that entered the bags from outside and $(P_0 - P_t)_{P-Gt}$ refers to the amount of P removed from the *Pi-Gt-sand* complex inside the mesh bags.

We then distinguished between the fraction of P that has been released associated to goethite dissolution $(P\ release)_{diss}$ and the fraction released by other mechanisms (i.e., competition of organic acid anions with P for the same adsorption sites), using the following equation:

$$(P\ release)_{diss} = (P_0 - P_0 \frac{Fe_t}{Fe_0}) \quad \text{(Eq.2)}$$

where $P_0 \frac{Fe_t}{Fe_0}$ is the amount of P still associated to goethite at time t. In this equation we assumed that P saturation of goethite remained constant, thus a change of Fe content after incubation in the soil is associated with a P loss associated to goethite dissolution.

The difference between *net P release* and $(P\ release)_{diss}$ was considered the fraction of P released by other mechanisms.

Statistical analysis

One-way ANOVA and regressions, to test the effects of age and substrate on the measured properties, were performed using the R 3.3.3 software (R Core Team, 2014). Tukey HSD was used to test differences at a significance level of $p < 0.05$, and the results were showed as boxplots using the multcomp R package (Hothorn et al., 2008).

Results

Soil properties along the two chronosequences

Soil properties changed along the two chronosequences with different intensity. pH decreased from 7.6 to 5.7 in mineral horizons along the S chronosequence, while it varied from 7.5 to 6.1 in the SG sites (Table 1). pH was lower in the organic horizons, from 5.8 to 5.0 in S sites and almost constant, around 5.8 in the SG sites.

In both chronosequences, total organic carbon (TOC) and total nitrogen (TN) contents were around zero in the barren sites and increased with age, with lower values in the S than in the SG chronosequence, especially in S190. Surprisingly, the highest TOC and TN contents were reached in S3000. Soil TOC/TN ratios were, as expected, higher under larch trees than in the barren S5 and SG5 sites, and they did not change significantly with soil age nor with parent material lithology, except in SG190 (much higher values on pure serpentinite). In the organic horizons under the larch trees, the TOC increased along the S chronosequence and decreased along the SG one, leading to greater TOC/TN values in S than in SG sites ($p<0.05$).

Cation exchange capacity (CEC), negligible at the beginning of soil formation, slightly increased with age reaching 11.9 $cmol_{(+)}\ kg^{-1}$ in the S3000 site, mainly due to accumulation of soil organic matter (Table 1). As expected, Mg was found to be the most abundant element in the exchange complex (35.7 ÷ 71.0%) in all sites, followed by Ca (23.1 ÷ 37.1%). The Ca/Mg ratio was <1 in most sites, with the highest value in the TOC-rich S3000 site (Ca/Mg=1.3). The low K values fell within the average range of exchangeable K in alpine soils, below 0.20 $cmol_{(+)}\ kg^{-1}$. Exchangeable Ni was quite high in all sites, with slightly greater values in the S sites than in the SG ones, reaching 20.7 mg kg^{-1} in S190.

The total phosphorus (TP) content of the mineral horizons ranged between 48.4 and 399 mg kg^{-1}, with the lowest values in the S chronosequence, especially in the 5- and 190-year-old sites. In the latter, TP was as low as 54.6 mg kg^{-1}. In the SG chronosequence, the inclusion of 10% gneiss resulted in a higher TP content, which ranged from 122 to 342 mg kg^{-1} (Table 1 and Figure 2a).

This led to increasing TOC/TP ratios with age, from 18.6 to 232 in the S sites whereas in the other chronosequence the highest TOC/TP ratio was reached in SG70 (75.6).

The changes observed in the mineral layers were reflected in the organic horizons where TP ranged only from 412 to 445 mg kg^{-1} in the S sites, compared to the much greater values reached in the SG sites (up to 1166 mg kg^{-1}). In organic horizons, TP was significantly higher in SG sites (ca. 20% of difference, $p<0.05$). In the few sites where it was possible to sample OL (fresh litter) and OH (completely altered organic material) horizons separately, much higher TP values were measured in OL (ca. 1500 mg kg^{-1}) than in OH ones (ca. 450 mg kg^{-1}).

Parallel to TP, the available P fraction (P_{av}) was extremely low, slightly increasing with age up to 12.0 mg kg^{-1} in S3000 (Figure 2b). The P_{av}/TP ratio increased linearly with age along the S chronosequence, while this trend was less visible on the SG one (Figure 2c).

Total iron (Fe_t) content in soil was rather constant in both chronosequences and ranged between 49.2 and 68.7 g kg^{-1}. Total magnesium was quite high (147-149 g kg^{-1}) in the youngest sites and decreased with age, more markedly in the SG than in the S sites. The same trend was observed for total nickel and chromium, although for these elements important differences were noticed between S5 and SG5.

Role of mycorrhizae on accessing P forms from Gt–sand systems

Ergosterol content

After 13 months of incubation in soil, in both chronosequences, similarly low values of ergosterol in all mesh bags systems were found in the 5-year-old sites. The values drastically increased with age, and in both S and SG sites; the colonization trend was in the order *Pi-Gt–sand* > *Gt–sand* ~ *InsP6-Gt–sand* ($p<0.05$, Figure 3). Though not significantly different, the highest average value of ergosterol in *Gt–sand* mesh bags was measured in S70 and SG70 (Figure 3a). Soil TP was marginally significantly negatively correlated with ergosterol in *Gt–sand* bags ($p=0.06$, $r=0.35$) in both chronosequences.

The ergosterol content in the *Pi-Gt–sand* systems showed a more significant trend with site age (Figure 3b). Despite the large variability, this was well visible in S sites (values decreasing from 0.59 in S190 to 0.29 mg kg^{-1}in S3000), and less marked in SG sites (from 0.35 to 0.24 mg kg^{-1}). The ergosterol content in these systems was significantly higher in S than in SG ($p<0.05$) and inversely correlated to soil TP ($r=0.41$, $p<0.05$).

In the *InsP6-Gt*–sand systems, the overall fungal colonization was lower compared to inorganic P. No significant differences were observed between S and SG sites. The decreasing trend with age was visible, though not significant, in SG sites. The values were between 0.40 and 0.11 mg kg^{-1} in all sites (Figure 3c).

Phosphorus content

After 13 months of incubation in soil, gross P inputs were observed in the *Gt-sand* systems, where the absence of P on the goethite surface allowed the evidence of P fluxes from the surrounding soil into the bags, with values ranging between 3.8 and 6.4 mg P kg^{-1} of *Gt-sand* in both chronosequences (data not shown). Even if quartz sand was acid-washed before preparation of the mesh bags, a residual P content of 1.5 mg kg^{-1} was found in the initial *Gt–sand* systems before soil incubation. The net P input was thus between 2.3 and 4.9 mg kg^{-1}. No clear increasing trends with soil age, nor a difference related to parent material lithological composition were detected (Figure 4a).

Net P outputs were instead observed in the P-containing systems. In particular, the highest P release occurred in the *Pi-Gt–sand* systems (Figure 4b). The net release of P was calculated as reported in Eq. 1, i.e. the difference between the sum of total P initially present in the mesh bags (Pi =18.19 mg kg^{-1}) and the input of P from surrounding environment measured in *Gt–sand* systems. Net P output increased from 6.2 to 13.9 mg P kg^{-1} of *Pi-Gt–sand* in S190 and then decreased to 11.5 mg P kg^{-1} in S3000. In the SG sites, the values in SG70, SG190 and SG 3000 were similar (between 8.7 and 10.7 mg P kg^{-1}). The net P output corresponded to 27-75% of total P in S sites, and to 16 to 58% in SG sites.

In *InsP6-Gt–sand* systems, the P release in S5 and SG5 was negligible and increased to 8.8 mg P kg^{-1} in S190, significantly correlated with site age on pure serpentinite ($p<0.05$, Figure 4c). In SG sites, the P release was slightly lower but not significantly correlated with site age.

Iron content

Before incubation in soil, the average iron (Fe) content in the *Gt–sand* systems was 5.05 g Fe kg^{-1}. After incubation, no Fe release was observed in the youngest sites, whereas in the 70-, 190- and 3000-year-old sites of both chronosequences, an output of Fe occurred, which slowly increased from younger to older sites (Figure 5a). The increase of Fe release with age was marginally significant in S sites ($p<0.1$), ranging from 2.76 to 2.98 g Fe kg^{-1} from S70 to S3000, and not

significantly influenced by soil age in SG sites, where we observed a release of 2.36-3.16 g Fe kg^{-1}. These values corresponded to 53-58% and 50-61% of total Fe contained in the mesh bags incubated in S and SG sites, respectively.

The Fe release from *Pi-Gt–sand* mesh bags was negligible in S5 and SG5 and did not vary consistently with site age, the highest value being measured in S190 and the lowest in SG190 (Figure 5b). A greater release (38-54% of initial Fe) was observed in S sites compared to SG sites (37-47% of initial Fe).

In the *InsP6-Gt–sand* systems, a significant increase in Fe release was measured in S and SG sites older than 5 years, with values increasing from 29 to 46% of initial Fe from S70 to S3000, and from 37 to 46% from SG70 to SG3000 (Figure 5c).

Release of P associated to goethite dissolution and by competition

Based on the previous data, we calculated the fraction of released P associated to goethite dissolution using Eq. 2. The P released from *Pi-Gt–sand* systems positioned in S sites was between 0.67 mg kg^{-1} and 9.69 mg kg^{-1}(Table 2), corresponding to 3.7-53% of initial P. The amount released from the systems in SG sites was lower ranging between 2.8 and 45% (Table 2).

In the *InsP6-Gt–sand* systems, the age trend was strongly visible ($p<0.05$) in the P fraction released with goethite in both S and SG sites, increasing from 0 to 45% of initial P (Table 2).

The remaining fraction of P was assumed to be removed from Gt-sand systems by competition with organic acid anions produced by ECM. This fraction was greater from Pi systems in S sites than in SG sites, representing 16 - 23% and 13 -16% of initial P, respectively. The fraction of InsP6 was quite lower, being 5-12 % in the S sites, and completely negligible in the SG sites, except SG5.

Discussion

Soil P dynamics in the two chronosequences

One of the most limiting factors on serpentinite ecosystems is the low P content, which is generally insufficient for guaranteeing vegetation development. The soils developed on pure serpentinite in the studied area (particularly where trees were absent) were characterized by TP levels <50 mg kg^{-1}, which represent the lowest values globally registered (Yang et al., 2013). As the pedogenesis and vegetation succession advance, plants, especially coniferous species, may overcome these hostile conditions by reducing the effect of the serpentine syndrome (Barton and Wallenstein, 1997;

Bonifacio et al., 2013; D'Amico et al., 2014; D'Amico et al., 2017). Carbon and nitrogen contents increased with soil age accumulating in the organic layers and becoming incorporated in the mineral horizon already after 70 years. Parallel to TOC and TN, TP increased in the organic layers and in the upper mineral horizon, as observed in different chronosequences (Crews et al., 1995; Bernasconi et al., 2011; Celi et al., 2013). The net increase of TP in the surface soil can be a consequence of P translocation from deeper to upper layers by plant uplift (Jobbágy and Jackson, 2001), providing evidence that the process is highly active even under hostile conditions. However, the extreme P scarcity in S sites limited the accumulation in the upper mineral horizons, which never reached 200 mg kg^{-1} even in the oldest site. The low values indicate that, though present for sure, dust inputs are not able to modify P contents significantly. Similarly, the TP content in the organic horizons of S sites remained on average 20% less than the amount accumulated in the SG sites. As a consequence, the TOC/TP ratios were always greater in the S with respect to the SG sites. This may be related not only to a lower incorporation of P in the organic material, but also to a slower decomposition of organic matter, as deduced also by the TOC/TN ratios. The low accumulation of TP in the surface mineral horizons may be due also to the subalkaline pH, which only slightly favoured the dissolution of P-bearing minerals. The strong acidifying effect of conifer litter observed commonly in vegetation chronosequences (i.e. Ritter et al. 2003; Cerli et al. 2006; Celi et al., 2013) could be here counteracted by the buffering effect of serpentine dissolution, releasing magnesium in the soil solution.

In the SG chronosequence, the small gneiss inclusions in the glacial till were sufficient to increase P levels from 200 to 400 mg kg^{-1} in the mineral horizon. Gneiss can be indeed six times richer in P than ultramafic rocks (Porder and Ramachandran, 2013). The initial greater content of TP in the substrate, together with a smaller Ni concentration, contributed to a faster vegetation colonization and to the relative accumulation of TP in the upper horizons, magnifying the plant uplift process.

Despite the lower TP accumulation, P biocycling was very active in the P-poorest soils, as evidenced by the P_{av}/TP ratio, which can be used as a marker of P biocycling. While this ratio was rather low and stable in the SG chronosequence, indicating that the slightly higher TP content was sufficient to feed the available P pool, it drastically increased along the S chronosequence. In this severely P-limited ecosystem, plants rely more on P biocycling rather than using P directly from P-bearing minerals (Richardson et al., 2011), creating a self-improving mechanism for P bioaccumulation and recycling with soil development. The positive correlation between P_{av} and TOC confirms the control of bioaccumulation to increase P efficiency (Stutter et al. 2015) of this ecosystem.

Role of mycorrhizae on accessing P forms from Gt-sand systems

Based on the above considerations, we investigated the capacity of mycorrhizae to explore soil for P acquisition by incubating mesh bags filled with inorganic and organic P forms adsorbed on goethite-sand systems.

Fungal colonization increased from about negligible to relatively high values along the two chronosequences, with greater amounts in the pure serpentinite chronosequence ($p<0.05$ in *Gt-sand* and *P-Gt-sand* systems). The mesh bags incubated in the youngest site of both chronosequences had minute amounts of fungal biomass, regardless of the P source. Conversely, the highest amount of ergosterol was observed in the 70-year-old site of both chronosequences, where sparse larch trees were present but available P was still low. Fungal biomass in the mesh bags in the older sites was probably dominated by ectomycorrizal fungi associated with larch trees since meshbags did not contain any substrate to grow on for saprotrophic fungi. Previous studies have shown that EMF are generally more abundant in the meshbags than other soil borne fungi (Hedh et al. 2008, Rosenstock et al. 2018, Wallander et al. 2010, Hagenbo et al. 2018) and mostly contribute to the fungal biomass in the meshbags (Hagenbo et al. 2018). According to Kałucka and Jagodziński (2017), mycorrhizal symbiosis seems to play an important role during the early stages of soil formation, when the weathering degree is still incipient and the nutrient status low. The higher fungal colonization generally observed in mesh bags incubated along the S chronosequence, in concomitance with the lower soil TP contents, confirmed that, in P-limited environments, EMF growth is enhanced due to the need of trees to allocate more carbon resources to increase P acquisition. Rosenstock et al. (2016) found out that P limitations in spruce forest soils, and, thus, host plant P demand, stimulate EMF growth: in their study, mesh bags incubated in serpentinite sites had a much higher ergosterol content, compared to mesh bags from less P-limiting amphibolite and granite soils. We found indeed a significant inverse correlation between soil TP and ergosterol content in both *Gt–sand* ($r=-0.38$, $p<0.05$) and *Pi-Gt–sand* ($r=-0.411$, $p<0.05$) mesh bags. The same inverse correlation with TP was found on different substrata in a spruce forest in south-western Sweden (Hedh et al. 2008), in a peatland in western Finland (Potila et al. 2009), and in a coniferous forest in New Zealand (Koele et al. 2014).

Parallel to EMF colonization, we observed a significant P release from the mesh bags, generally increasing with soil age, except from S5 and SG5 sites, where only a slight release was measured. In these barren sites with no potential EMF hosts, P was probably lost by the action of weak rainfall acidity. The low P release measured here highlights also that the removal of P from mesh bags by physical and chemical processes could be considered negligible throughout all sites, since these

processes, if occurring, should have been particularly expressed in S5 and SG5, characterized by a coarse material and absence of vegetation cover (Celi et al., 2013). The contemporary negligible release of Fe from *Gt–sand*, *Pi-Gt–sand*, and *InsP6-Gt–sand* systems in S5 and SG5 not only ruled out leaching, but also particle dispersion and migration of goethite nanoparticles out of the mesh bags.

Where larch trees were growing, P was released in greater amounts from mesh bags incubated in the S sites compared to SG sites and, between P forms, inorganic P was released more than InsP6. The generally greater release of Pi from mesh bags incubated in the pure serpentinite sites, together with the ergosterol trend, is an evidence that EMF could potentially mine more Pi from goethite where the surrounding P availability is lower (Rosenstock et al. 2016). However, several studies have suggested that EMF are able to dissolve minerals too, exclusively to obtain nutrients (Smits and Wallander, 2017), suggesting that dissolution of goethite may be a consequence of nutrient requirements. This may justify why the release of Fe from *Pi-Gt–sand* systems was negligible in the youngest sites and increased in the colonized mesh bags, similarly to Pi release. Mineral dissolution may occur by chelation of Fe^{3+} from goethite through fungal exudation of organic acid anions and siderophores (Casarin et al., 2004; Rosling and Rosenstock, 2008; Adeleke et al., 2012) or reduction of Fe^{3+} to Fe^{2+} (Parfitt, 1979; Marschner et al. 2011) probably through exudation of electron donor compounds such as phenolic compounds (Krumida, 2018) .

The release of Pi connected with goethite dissolution ranged between 2.8 ÷ 54% of the total P present before incubation (Table 2), representing more than 14-78% of the total released fraction and without differences between the two chronosequences.

Pi detachment from goethite can also be achieved by exudation of protons and organic acids through competition with phosphate for the same adsorption sites (Richardson et al. 2011). Thus, the remaining fraction of Pi could have been released from *Pi-Gt–sand* systems by this mechanism. This fraction showed significant differences between the two chronosequences, with higher values in S sites (15.9 ÷ 23.0%) than in the SG ones (12.7 ÷ 18.3%). In the fertility-poorer S chronosequence, EMF could be more active in producing organic acid anions that may compete with inorganic P for the same sorption sites.

The good correlation between the P fraction released within goethite dissolution and ergosterol ($p<0.05$) in S sites may suggest a key role of mycorrhizae, which adopt the production of organic acids or siderophores/e^- donor compounds to dissolve goethite as the main strategy for P uptake.

However, goethite dissolution occurred also in *Gt–sand* systems along the two chronosequences. Shah et al. (2015) demonstrated that EMF may reduce Fe^{3+} during organic matter decomposition to obtain N. Thus, EMF-mediated Fe reduction can also be related to other nutrients uptake. In

addition, the fact that Fe release was observed in all sites with larch trees and well-developed litter layers may not exclude a migration of plant derived organic acids and phenols into mesh bags positioned in the mineral layers and their contribution to goethite dissolution. In addition, when working in field conditions other microorganisms are usually present in the system (Jones and Smith, 2004), suggesting a complex interaction of mycorrhizae and other microorganisms with plants in mining P recalcitrant sources.

Inositol phosphate was released in lower amounts compared to Pi, and less related to soil P status and type of lithology. Jansa et al. (2011) reviewed several works that demonstrate the capacity of EMF to produce enzymes that can hydrolize organic P substrates. Myers and Leake (1996) showed that EMF can use phosphodiesters as sole P source without the intervention of saprotrophs. Colpaert et al. (1997) evaluated the utilization of inositol hexaphosphate by EMF fungi, demonstrating substantial extracellular acid phosphatase activity associated with mycelial biomass and increased P nutrition of the mycorrhizal plants. However, when InsP6 is adsorbed onto Fe oxide surfaces, such as in our study, it forms stable complexes and this interaction led to a selective accumulation of inositol phosphates in most soils and sediment environments, with respect to other more labile P forms (Magid et al., 1996). George et al. (2007) and Giaveno et al. (2010) showed that phytases could not hydrolyze InsP6, once it is sorbed on soil and Fe oxides, such as goethite. The capacity of EMF to use this P source is thus conditional to mechanisms that can detach first the molecule from the Fe (hydr)oxide. However, the sole action of competitive compounds, such as H^+ and organic acid anions was apparently low and accounted for only 5-12% of the total P released from the *InsP6-Gt-sand* systems. This is in agreement with previous works that show a limited extraction of InsP6 from iron oxides at pH 3.5-4.5 and by citrate (Celi et al., 2003, Martin et al., 2004). In addition, Martin et al. (2004) showed a low P acquisition in plants grown with InsP6 as only P source. The main P release was instead parallel to goethite dissolution and less related to lithology, accounting for 34-44% of the total P retained from the *InsP6-Gt-sand* systems. It can be thus inferred that the high capacity of EMF to release P as a consequence of Fe oxide dissolution, as invoked for Pi, may be strategic also for the utilization of such a highly stabilized P form. Although we cannot exclude other processes that can favour P detachment from goethite, such as fluxes of plant-derived organic compounds, the limited use of inositol phosphate sorbed onto goethite in soils by non-mycorrhizal plants (George et al 2007; Martin et al., 2004) may support the role of EMF in InsP6 release. Aside from the abovementioned mechanisms, this may be due to indirect effects of EMF on other components of the system involved in P cycling, such as bacteria and saprotrophytic fungi (Tibbett and Sanders, 2002).

CONCLUSIONS

This work shows the main P dynamics in soils developed along two alpine chronosequences in a glacier forefield, dominated by serpentinite lithology. The extremely P-poor soils, particularly in the western chronosequence, together with other harsh conditions, drastically slowed down the encroachment by vegetation and the primary succession.

In such hostile edaphic conditions for plant development, the symbiosis of larch with mycorrhizal fungi was found to be extremely important, particularly in the chronosequence characterized by low P availability on pure serpentinite, as shown by the high EMF growth in these sites. Ericoid mycorrhizae cannot be excluded as well in a few samples taken from S3000 and, to a lesser extent, SG3000. EMF were able to release both inorganic and organic P forms adsorbed onto goethite, likely adopting combined mechanisms. The release of P parallel to goethite dissolution led to hypothesize a production of specific metabolites by EMF, which seemed a strategic mechanism especially for the release of inositol phosphates. The greater affinity of this organic P form for the oxides with respect to inorganic P leads indeed to the formation of stable complexes, hardly affected by the action of organic acid anions. Conversely, the latter seemed particularly efficient for releasing inorganic P in the pure serpentinite sequence . However, the relevance of these results needs to be further investigated for better identifying the mechanisms of P release and understanding the acquisition of P by EMF and associated host plants from inositol phosphates.

References

Adeleke RA, Cloete TE, Bertrand A, Khasa DP (2012). Iron ore weathering potentials of ectomycorrhizal plants. Mycorrhiza 22(7):535-544.

Almeida JP. 2019. Biomass, community structure and phosphorus uptake of ectomycorrhizal fungi in response to phosphorus limitation and nitrogen deposition. Doctoral thesis. Department of Biology. Lund University.

Barton AM, Wallenstein MD (1997) Effects of invasion of Pinus virginiana on soil properties in serpentine barrens in southeastern Pennsylvania. J. Torrey Bot Soc 124(4):297-305

Bernasconi SM, Bauder A, Bourdon A, Brunner I, Bünemann E, Christl I, Derungs N, Edwards P, Farinotti D, Frey B, Frossard E, Furrer G, Gierga M, Göransson H, Gülland K, Hagedorn F, Hajdas I, Hindshaw R, Ivy-Ochs S, Jansa J, Kiczka M, Kretschmar R, Lemarchand E, Luster J, Magnusson J, Mitchell EAD, Venterink HO, Plötze M, Reynolds B, Smittenberg RH, Stähli M, Tamburini F, Tipper ET, Wacker L, Welc M, Wiederhold JG, Zeyer J, Zimmermann S, Zumsteg A (2011)

Chemical and biological gradients along the Damma Glacier soil chronosequence, Switzerland. Vadose Zone J 10:867–883

Berner C, Johansson T, Wallander H (2012) Long-term effect of apatite on ectomycorrhizal growth and community structure. Mycorrhiza 22:615-621

Bonifacio E, Falsone G, Catoni M (2013) Influence of serpentine abundance on the vertical distribution of the available elements in soil. Plant Soil 368:493-506

Brooks RR (1987) Serpentine and its vegetation: a multidisciplinary approach. Dioscorides, Oregon

Bucher M (2007) Functional biology of plant phosphate uptake at root and mycorrhiza interfaces. New Phytol 173:11-26

Burga CA, Krüsi B, Egli M, Wernli M, Elsener S, Ziefle M, Fischer T, Mavris C (2010) Plant succession and soil development on the foreland of the Morteratsch glacier (Pontresina, Switzerland): straight forward or chaotic? Flora 205:561–576

Cairney JW (2011). Ectomycorrhizal fungi: the symbiotic route to the root for phosphorus in forest soils. Plant Soil 344: 51-71.

Casarin V, Plassard C, Hinsinger P, Arvieu JC (2004) Quantification of ectomycorrhizal fungal effects on the bioavailability and mobilization of soil P in the rhizosphere of Pinus pinaster. New Phytol 163(1):177-185

Celi L, Lamacchia S, Ajmone-Marsan F, Barberis E (1999) Interaction of inositol hexaphosphate on clays: adsorption and charging phenomena. Soil Sci 164(8):574-585

Celi L, Presta M, Ajmone-Marsan F, Barberis E (2001) Effects of pH and electrolytes on inositol hexaphosphate interaction with goethite. Soil Sci Soc Am J 65(3):753-760

Celi L, De Luca G., Barberis E (2003) Effects of interaction of organic and inorganic P with ferrihydrite and kaolinite- iron oxide systems on iron release. Soil Sci 168(7):479-488

Celi L, Cerli C, Turner BL, Santoni S, Bonifacio E (2013) Biogeochemical cycling of soil phosphorus during natural revegetation of Pinus sylvestris on disused sand quarries in Northwestern Russia. Plant Soil 367:121-134

Cerli C, Celi L, Johansson MB, Kögel-Knabner I, Rosenqvist L, Zanini E (2006) Soil organic matter changes in a spruce chronosequence on Swedish former agricultural soil I. Carbon and lignin dynamics. Soil Sci 171: 837-849

Colpaert JV, Van Laere A, Van Tichelen KK, Van Assche JA (1997) The use of inositol hexaphosphate as a phosphorus source by mycorrhizal and non-mycorrhizal Scots Pine (Pinus sylvestris). Funct Ecol 11:407-415

Courty PE, Buée M, Diedhiou AG, Frey-Klett P, Le Tacon F, Rineau F, Turpault M-P, Uroz S, Garbaye J (2010) The role of ectomycorrhizal communities in forest ecosystem processes: New perspectives and emerging concepts. Soil Biol Biochem 42:679-698

Crews TE, Kitayama L, Fownes JH, Herbert DA, Mueller-Dombois D, Vitousek PM (1995) Changes in soil phosphorus fractions and ecosystem dynamics across a long chronosequence in Hawaii. Ecology 76(5):1407-1424

Darch T, Blackwell MSA, Hawkins JMB, Haygarth PM, Chadwick D (2014) A Meta-Analysis of Organic and Inorganic Phosphorus in Organic Fertilizers, Soils, and Water: Implications for Water Quality. Critical Rev Env Sci Techn 44(19):2172-2202

D'Amico ME, Bonifacio E, Zanini E (2014) Relationships between serpentine soils and vegetation in a xeric inner-Alpine environment. Plant Soil 376:111-128

D'Amico ME, Freppaz M, Leonelli G, Bonifacio E, Zanini E (2015) Early stages of soil development on serpentinite: the proglacial area of the Verra Grande Glacier, Western Italian Alps. J Soils Sediments 15:1292-1310

D'Amico ME, Freppaz M, Zanini E, Bonifacio E (2017) Primary vegetation succession and the serpentinite syndrome: the proglacial area of the Verra Grande glacier, North-Western Italian Alps. Plant Soil 415:283-298

Fang Z, Shao C, Meng Y, Wua P, Chen M (2009) Phosphate signaling in Arabidopsis and Oryza sativa. Plant Sci 176:170-180

George TS, Giles CD, Menezes-Blackburn D, Condron LM, Gama-Rodrigues AC, Jaisi D, Lang F, Neal AL, Stutter MI, Almeida DS, Bol R, Cabugao KG, Celi L, Cotner JB, Feng G, Goll DS, Hallama M, Krueger J, Plassard C, Rosling A, Darch T, Fraser T, Giesler R, Richardson AE, Tamburini F, Shand CA, Lumsdon DG, Zhang H, Blackwell MSA, Wearing C, Mezeli MM, Almås ÅR, Audette Y, Bertrand I, Beyhaut E, Boitt G, Bradshaw N, Brearley CA, Bruulsema TW, Ciais P, Cozzolino V, Duran PC, Mora ML, de Menezes AB, Dodd RJ, Dunfield K, Engl C, Frazão JJ, Garland G, González Jiménez JL, Graca J, Granger SJ, Harrison AF, Heuck C, Hou EQ, Johnes PJ, Kaiser K, Kjær HA, Klumpp E, Lamb AL, Macintosh KA, Mackay EB, McGrath J, McIntyre C, McLaren T, Mészáros E, Missong A, Mooshammer M, Negrón CP, Nelson LA, Pfahler V, Poblete-Grant P, Randall M, Seguel A, Seth K, Smith AC, Smits MM, Sobarzo JA, Spohn M, Tawaraya K, Tibbett M, Voroney P, Wallander H, Wang L, Wasaki J, Haygarth PM (2018) Organic phosphorus in the terrestrial environment: A perspective on the state of the art and future priorities. Plant Soil 427:191-208

George TS, Simpson RJ, Gregory PJ, Richardson AE (2007) Differential interaction of Aspergillus niger and Peniophora lycii phytases with soil particles affects the hydrolysis of inositol phosphates. Soil Biol Biochem 39(3)793-803

Giaveno C, Celi L, Richardson AE, Simpson RJ, Barberis E (2010) Interaction of phytases with minerals and availability of substrate affect the hydrolysis of inositol phosphates. Soil Biol Biochem 42(3):491-498

Hagenbo A, Kyaschenko J, Clemmensen K E, Lindahl B. D, Fransson P (2018). Fungal community shifts underpin declining mycelial production and turnover across a Pinus sylvestris chronosequence. J Ecol 106: 490-501.

Hammond JP, White PJ (2008) Sucrose transport in the phloem: integrating root responses to phosphorus starvation. J Expl Bot 59:93-109

Harley JL, Smith SE (1983) Mycorrhizal symbiosis. Academic, New York.

Hedh J, Wallander H, Erland S (2008) Ectomycorrhizal mycelial species composition in apatite amended and non-amended mesh bags buried in a phosphorus-poor spruce forest. Mycol Res 112(6):681-688

Hothorn T, Bretz F, Westfall P (2008) Simultaneous inference in general parametric models. Biom J 50(3):346–363

IUSS Working Group WRB (2015) World reference base for soil resources 2015, World Soil Resources Reports, No 103, FAO, Rome

Jansa J, Finlay R, Wallander H, Smith FA, Smith SE (2011) Role of mycorrhizal symbiosis in phosphorus cycling. In: Bünemann et al. (Eds.) Phosphorus in action, Springer-Verlag, 137-168

Jobbágy EG, Jackson RB (2001) The distribution of soil nutrients with depth: Global patterns and the imprint of plants. Biogeochemistry 53(1):51-77

Jones MD, Smith SE (2004) Exploring functional definitions of mycorrhizas: are mycorrhizzas always mutualism? Can J Bot 82(8):1089-1109

Kałucka IL, Jagodziński AM (2017) Ectomycorrhizal Fungi: A Major Player in Early Succession. In: A. Varma et al. (eds.), Mycorrhiza - Function, Diversity, State of the Art; pp 187-229.

Koele N, Dickie IA, Blum JD, Gleason JD, de Graaf L (2014) Ecological significance of mineral weathering in ectomycorrhizal and arbuscular mycorrhizal ecosystems from a field-based comparison. Soil Biol Biochem 69:63-70

Landerweert R, Hoffland E, Finlay RD, Kuyper TW, Van Breemen N (2001) Linking plants to rocks: ectomycorrhizal fungi mobilize nutrients from minerals. Trends in Ecol Evol 16:248-254

Louche J, Ali MA, Cloutier-Hurteau B, Sauvage FX, Quiquampoix H, Plassard C (2010) Efficiency of acid phosphatases secreted from the ectomycorrhizal fungus Hebeloma cylindrosporum to hydrolyse organic phosphorus in podzols. FEMS Microbiol Ecol 73(2):323-335

Lynch JP, Brown KM (2008) Root strategies for phosphorus acquisition. In: White PJ, Hammond JP (Eds) The ecophysiology of plant-phosphorus interactions, Springer, 83-116

Magid J, Tiessen H, Condron LM (1996) Dynamics of organic phosphorus in soils under natural and agricultural ecosystems. In: Piccolo, A. (Ed), Humic substances in terrestrial ecosystems. Elsevier Science, Amsterdam, pp 429-466

Martin M, Celi L, Barberis E (1999) Determination of low concentrations of organic phosphorus in soil solution. Commun Soil Sci Plant Anal 30(13-14):1909-1917

Martin M, Celi L, Barberis E (2004) Desorption and plant availability of myo-inositol hexaphosphate adsorbed on goethite. Soil Sci 169(2):115-124

Mercalli L (2003) Atlante climatico della Valle d'Aosta, Società Meteorologica Italiana (ed), Torino

Myers MD, Leake JR (1996) Phosphodiesters as mycorrhizal P sources. II. Ericoid mycorrhiza and the utilization of nuclei as a phosphorus and nitrogen source by Vaccinium macrocarpon. New Phytol 132(3):445-451

Ohno T, Zibilske LM (1991) Determination of low concentration of phosphorus in soil extracts using malachite green. Soil Sci Soc Am J 55:892-895

Olsen S, Cole C, Watanabe F, Dean L (1954) Estimation of available phosphorus in soils by extraction with sodium bicarbonate. USDA Circular Nr 939, US Gov. Print. Office, Washington, D.C.

Parfitt RL (1979) The availability of P from phosphate-goethite bridging complexes. Desorption and uptake by ryegrass. Plant Soil 53: 55-65.

Plassard C, Louche J, Ali MA, Duchemin M, Legname E, Cloutier-Hurteau, B (2011) Diversity in phosphorus mobilisation and uptake in ectomycorrhizal fungi. Annals of Forest Science 68: 33-43.

Porder S, Ramachandran S (2013) The phosphorus concentration of common rocks – a potential driver of ecosystem P status. Plant Soil 367:41-55

Potila H, Wallander H, Sarjala T (2009) Growth of ectomycorrhizal fungi in drained petland forests with variable P and K availability. Plant Soil 316(1-2):139-150

R Core Team (2014) R: A language and environment for statistical computing. R Foundation for Statistical Computing, Vienna, Austria. URL http://www.R-project.org/

Rajakaruna N, Boyd RS (2008) The edaphic factor. In: Jorgensen SE, Fath B. (Eds) Enciclopedia of Ecology. Vol. 2. pp. 1201–1207

Read DJ, Perez-Moreno J. (2003) Mycorrhizas and nutrient cycling in ecosystems: a journey towards relevance? New Phytol 157:475-492

Richardson AE, Lynch JP, Ryan PR, Delhaize E, Smith FA, Smith SE, Harvey PR, Ryan MH, Veneklaas EJ, Lambers H, Oberson A, Culvenor RA, Simpson RJ (2011) Plant and microbial strategies to improve the phosphorus efficiency of agriculture. Plant Soil 349(1-2):121-156

Ritter E, Vesterdal L, Gundersen P (2003) Changes in soil properties after afforestation of former intensively managed soils with oak and Norway spruce. Plant Soil 249:319-330

Rosenstock NP, Berner C, Smits MM, Kram P, Wallander H. (2016) The role of phosphorus, magnesium and potassium availability in soil fungal exploration of mineral nutrient sources in Norway spruce forests. New Phytol 211:542-553

Rosenstock N, Ellström M, Oddsdottir E, Sigurdsson B. D, Wallander H (2019). Carbon sequestration and community composition of ectomycorrhizal fungi across a geothermal warming gradient in an Icelandic spruce forest. Fungal Ecology 40: 32-42.

Rosling A, (2009) Trees, Mycorrhiza and Minerals –Field relevance of in vitro experiments. Geomicr J 26(6):389-401

Rosling A, Rosenstock N (2008). Ectomycorrhizal fungi in mineral soil. Min Maga 72(1):127-130

Schwertmann U, Cornell RM (1964) Goethite, in: Iron oxides in laboratory: preparation and characterization, Part 2. Wiley-VCH, 64-65

Shah F, Schwenk D, Nicolas C, Persson P, Hoffmeister D, Tunlid A. (2015) Involutin is an Fe3+ reductant secreted by the ectomycorrhizal fungus Paxillus involutus during fenton-based decomposition of organic matter. Appl Env Microbiol 81:8427-8433

Smith SE, Read DJ (2008) Mycorrhizal symbiosis, 3rd ed. Academic, New York.

Smith SE, Anderson IC, Smith FA (2018) Mycorrhizal associations and phosphorus acquisition: from cells to ecosystems. In: Roberts JA (Ed.) Annual Plant Reviews online. doi:10.1002/9781119312994.apr0529

Smits MM, Wallander H (2017) Role of mycorrhizal symbiosis in mineral weathering and nutrient mining from soil parent material, in: Mycorrhizal Mediation of Soil Fertility, Structure, and Carbon Storage, edited by Johnson, N. C., Gehring, C., and Jansa, J.: Elsevier, Amsterdam. 35-46. ISBN:978-0-12-8043127, 2017.

Stutter MI, Shand CA, George TS, Blackwell MSA, Dixon L, Bol R, MacKay RL, Richardson AE, Condron LM, Haygarth PM (2015). Land use and soil factors affecting accumulation of phosphorus species in temperate soils. Geoderma 257-258:29-39

Sumner ME, Miller WP (1996) Cation exchange capacity and exchange coefficients, in: Sparks et al. (Eds.) Methods of soil analysis, Part 3, Chemical Methods, pp 1201-1229

Tibbett M, Sanders FE (2002) Ectomycorrhizal symbiosis can enhance plant nutrition through improved access to discrete organic nutrient parches of high resource quality. Ann Bot 89(6):783-789

Vergnano Gambi O, Gabbrielli R (1981) La composizione minerale della vegetazione degli affioramenti olofitici dell'alta Valle d'Ayas. Rev Valdôtaine Hist Nat 35:51-61

Vergnano Gambi O, Pedani R, Gabbrielli R (1987) Ulteriori dati sulla composizione minerale della vegetazione degli affioramenti ofiolitici della Valle d'Ayas. Rev Valdôtaine Hist Nat 41:99-100

Wallander H, Nilsson LO, Hagerberg D, Bååth E (2001) Estimation of the biomass and seasonal growth of external mycelium of ectomycorrhizal fungi in the field. New Phytol 151(3):753-760

Wallander H, Johansson U, Sterkenburg E, Brandström Durling M, Lindahl BD (2010). Production of ectomycorrhizal mycelium peaks during canopy closure in Norway spruce forests. New Phytologist 187(4): 1124-1134.

Wallander H, Ekblad A, Godbold DL, Johnson D, Bahr A, Baldrian A, Björk RG, Kieliszewska-Rokicka B, Kjøller R, Kraigher H, Plassard C, Rudawska M (2013) Evaluation of methods to estimate production, biomass and turnover of ectomycorrhical mycelium in forest soils – a review. Soil Biol Biochem 57:1034-1047

White PJ, Broadley MR, Greenwood DJ, Hammond JP (2005) Genetic modifications to improve phosphorus acquisition by roots. Proceedings 568, International Fertiliser Society, York

White PJ, Hammond JP (2008) Phosphorus nutrition of terrestrial plants. In: White PJ Hammond JP (Eds.) The ecophysiology of plant-phosphorus interactions. Springer, pp 51-81

Yan Y, Li W, Yang J, Zheng A, Liu F, Feng X, Sparks DL (2014) Mechanism of myo-inositol hexakisphosphate sorption on amorphous aluminum hydroxide: Spectroscopic evidence for rapid surface precipitation. Environ Sci Technol 48(12):6735-6742

Yang X, Post WM, Thornton PE, Jain A (2013) The distribution of soil phosphorus for global biogeochemical modelling. Biogeosciences 10:2525-2537

Figure captions

Fig. 1 Location of the Verra Grande glacier forefield and the samples sites.

Fig. 2 Phosphorus forms in the soils along the two chronosequences: total P, TP (a); available P, Pav (b); and the ratio between the available fraction and the total P content, Pav/TP (c). The letters above the boxes evidence significant differences.

Fig. 3 Ergosterol content in the *Gt-sand* (a), *Pi-Gt-sand* (b) and *InsP6-Gt-sand* (c) systems positioned between the organic and surface mineral soil horizons along the serpentinite chronosequence (S5, S70, S190 and S3000) and the serpentinite + 10% gneiss chronosequence (SG5, SG70, SG190 and SG3000). The letters above the boxes evidence significant differences.

Fig 4 The net phosphorus content released from the *Gt-sand* (a), *Pi-Gt-sand* (b) and *InsP6-Gt-sand* (c) systems positioned between the organic and surface mineral soil horizons along the serpentinite chronosequence (S5, S70, S190 and S3000) and the serpentinite + 10% gneiss chronosequence (SG5, SG70, SG190 and SG3000). The letters above the boxes evidence significant differences.

Fig.5 Iron released from the *Gt-sand* (a), *Pi-Gt-sand* (b) and *InsP6-Gt-sand* (c) systems positioned between the organic and surface mineral soil horizons along the serpentinite chronosequence (S5, S70, S190 and S3000) and the serpentinite + 10% gneiss chronosequence (SG5, SG70, SG190 and SG3000). The letters above the boxes evidence significant differences.

Tab. 1 *Main chemical properties of organic (where present) and surface mineral soil horizons along the serpentinite chronosequence (S5, S70, S190 and S3000) and the serpentinite + 10% gneiss chronosequence (SG5, SG70, SG190 and SG3000).*

Site	Horizon	pH	Fe_t	Mg_t	Ni_t	Cr_t	CEC	K_{ex}	Mg_{ex}	Ca_{ex}	Ni_{ex}	TOC	TN	TP	TOC/TN	TOC/TP
			---g kg^{-1}---		---mg kg^{-1}---		----------cmol$_{(+)}$ kg^{-1}----------				mg kg^{-1}	---g kg^{-1}---		mg kg^{-1}		
S5	C	7.6	62.5	149	1422	1229	0.49	0.01	0.30	0.10	2.62	0.9	0.08	48.4	11.2	18.6
S70	O	5.8	-	-	-	-	-	-	-	-	-	327	10.8	794	30.3	412
	AC	6.5	68.7	142	1249	1318	2.28	0.04	0.91	0.69	15.7	8.5	0.4	119	21.2	71.4
S190	O	5.2	-	-	-	-	-	-	-	-	-	371	10.5	670	35.4	554
	A	6.6	64.9	139	1358	1268	2.55	0.14	1.09	0.67	20.7	7.9	0.36	54.6	21.9	144
S3000	O	5.0	-	-	-	-	-	-	-	-	-	389	13.3	875	29.3	445
	A	5.7	63.8	138	884.2	1363	11.9	0.19	4.84	3.15	4.22	39.5	1.8	170	21.9	232
SG5	C	7.5	65.4	147	1358	1316	0.42	0.01	0.30	0.12	2.40	1.2	0.08	122	15.0	9.84
SG70	O	5.8	-	-	-	-	-	-	-	-	-	359	11.1	907	32.2	394
	A	6.8	67.1	147	1294	1232	2.79	0.05	1.56	1.19	8.14	10.1	0.5	133	20.2	75.6
SG190	O	5.9	-	-	-	-	-	-	-	-	-	333	16.7	1166	19.9	285
	A	6.7	53.6	89.3	914.1	1070	5.13	0.09	2.58	1.89	2.78	19.5	1.4	399	13.9	48.9
SG3000	O	5.7	-	-	-	-	-	-	-	-	-	330	12.9	966	25.6	341
	A	6.1	49.2	94.5	739.0	974.4	4.40	0.05	2.68	1.22	0.90	14.1	0.7	342	20.1	41.2

Tab. 2 *Calculated fractions of P released following goethite dissolution and by other mechanisms from Pi-Gt – sand and InsP6-Gt – sand systems positioned between the organic and surface mineral soil horizons along the serpentinite chronosequence (S5, S70, S190 and S3000) and the serpentinite + 10% gneiss chronosequence (SG5, SG70, SG190 and SG3000).*

		Pi-Gt – sand systems				InsP6-Gt – sand systems			
Lithology	**site (yrs)**	**P released with goethite (mg kg^{-1})**		**P released by other mechanisms (mg kg^{-1})**		**P released with goethite (mg kg^{-1})**		**P released by other mechanisms (mg kg^{-1})**	
Serpentinite	5	0.67	a	5.46	b	0.00	a	1.97	a
	70	7.83	b	2.89	ab	6.22	b	1.05	a
	190	9.69	c	3.91	ab	6.56	b	2.24	a
	3000	8.22	bc	3.45	ab	7.97	b	0.00	a
Serpentinite + 10%gneiss	5	0.51	a	2.43	a	0.00	a	2.14	a
	70	7.05	b	2.96	ab	6.33	b	0.00	a
	190	6.57	b	3.32	ab	6.49	b	0.00	a
	3000	8.25	bc	2.31	a	8.17	b	0.00	a

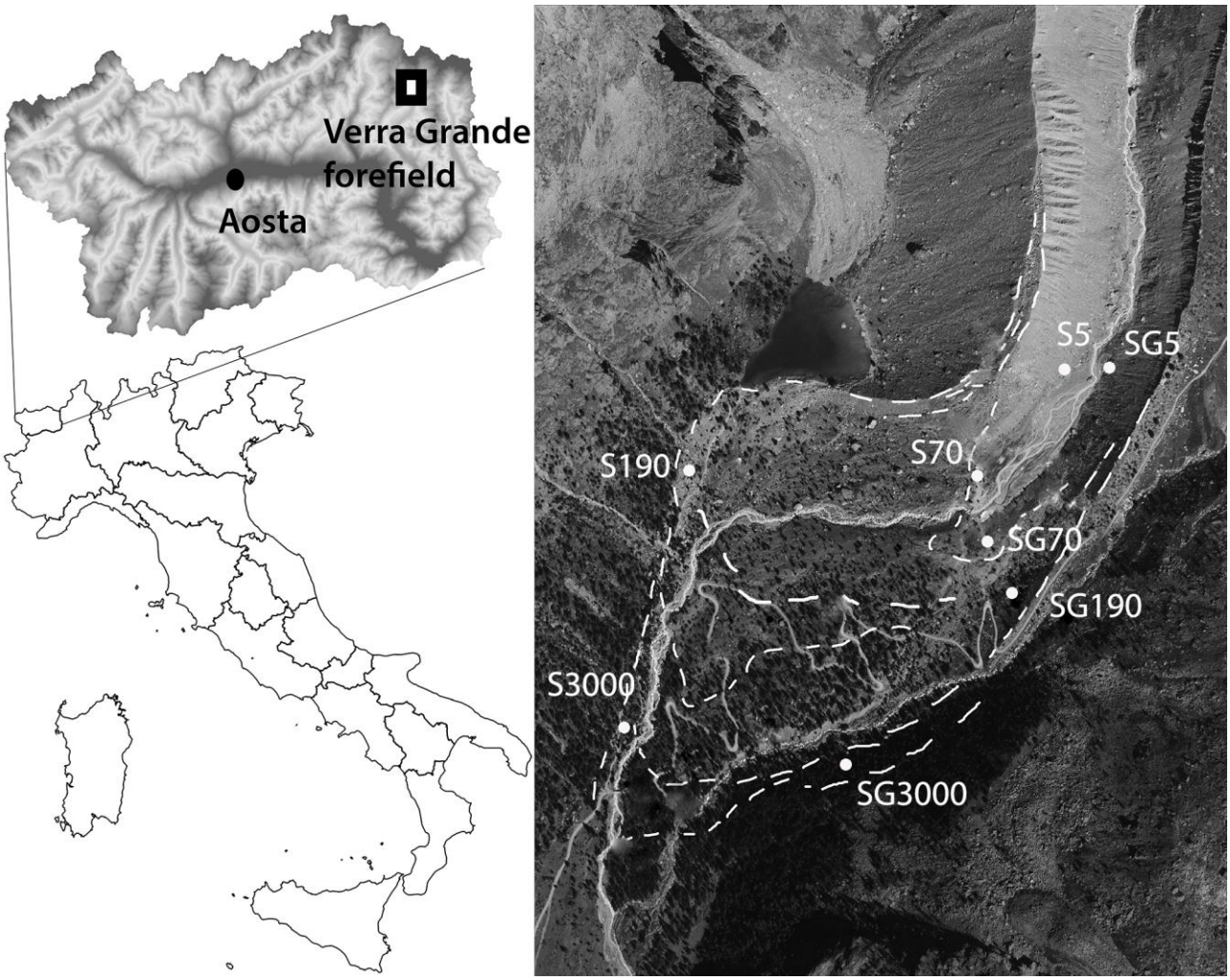

Fig. 1 Location of the Verra Grande glacier forefield and the samples sites.

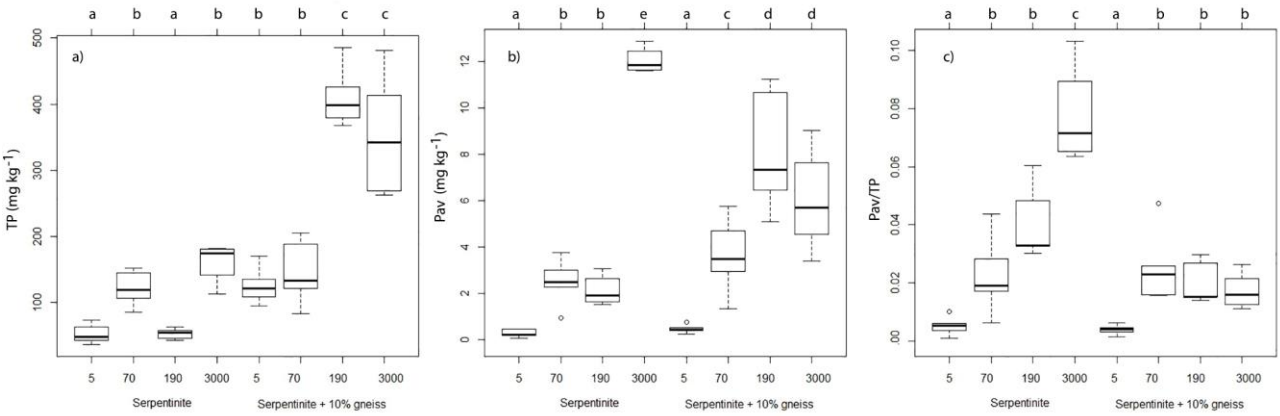

Fig. 2 Phosphorus forms in the soils along the two chronosequences: total P, TP (a); available P, Pav (b); and the ratio between the available fraction and the total P content, Pav/TP (c). The letters above the boxes evidence significant differences.

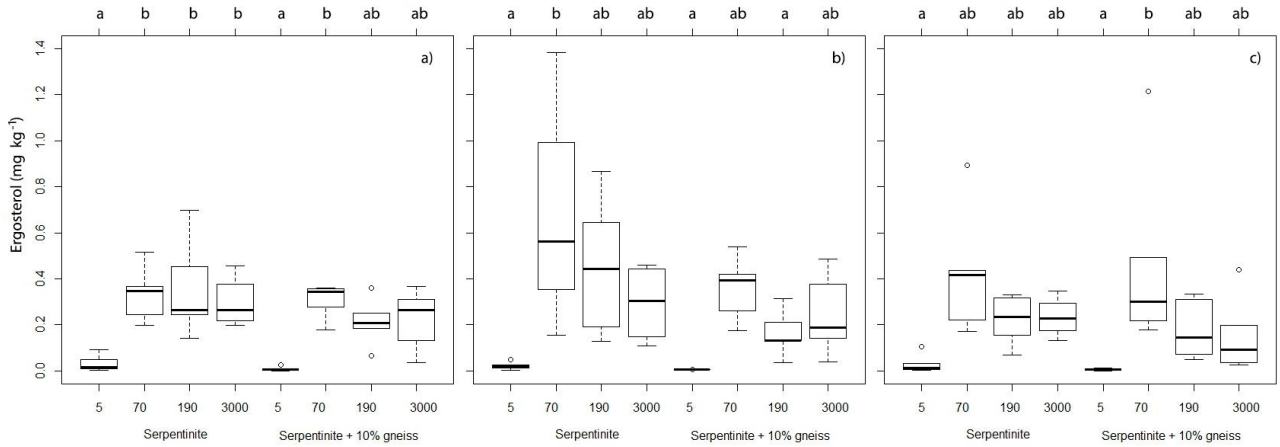

Fig. 3 Ergosterol content in the *Gt-sand* (a), *Pi-Gt-sand* (b) and *InsP6-Gt-sand* (c) systems positioned between the organic and surface mineral soil horizons along the serpentinite chronosequence (S5, S70, S190 and S3000) and the serpentinite + 10% gneiss chronosequence (SG5, SG70, SG190 and SG3000). The letters above the boxes evidence significant differences.

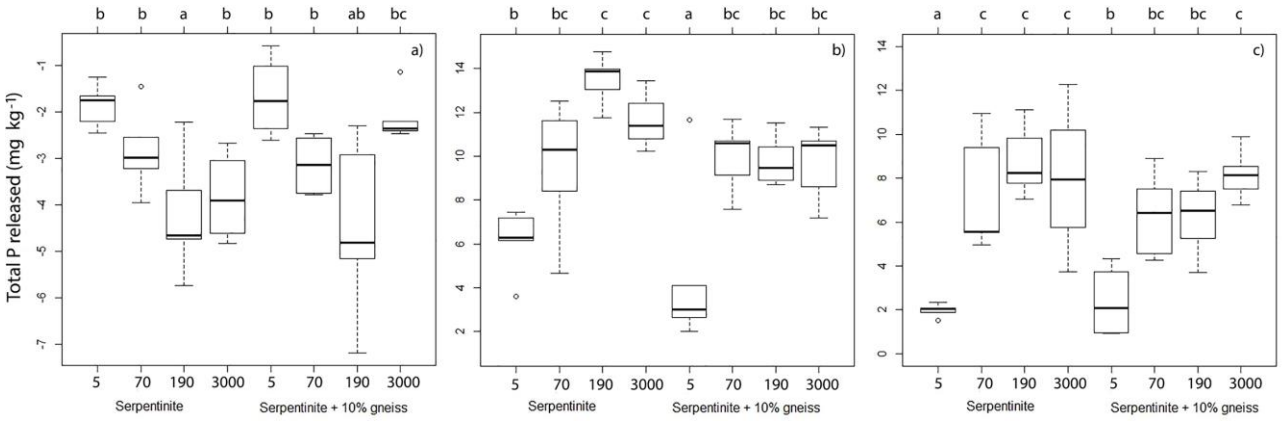

Fig 4 The net phosphorus content released from the *Gt-sand* (a), *Pi-Gt-sand* (b) and *InsP6-Gt-sand* (c) systems positioned between the organic and surface mineral soil horizons along the serpentinite chronosequence (S5, S70, S190 and S3000) and the serpentinite + 10% gneiss chronosequence (SG5, SG70, SG190 and SG3000). The letters above the boxes evidence significant differences.

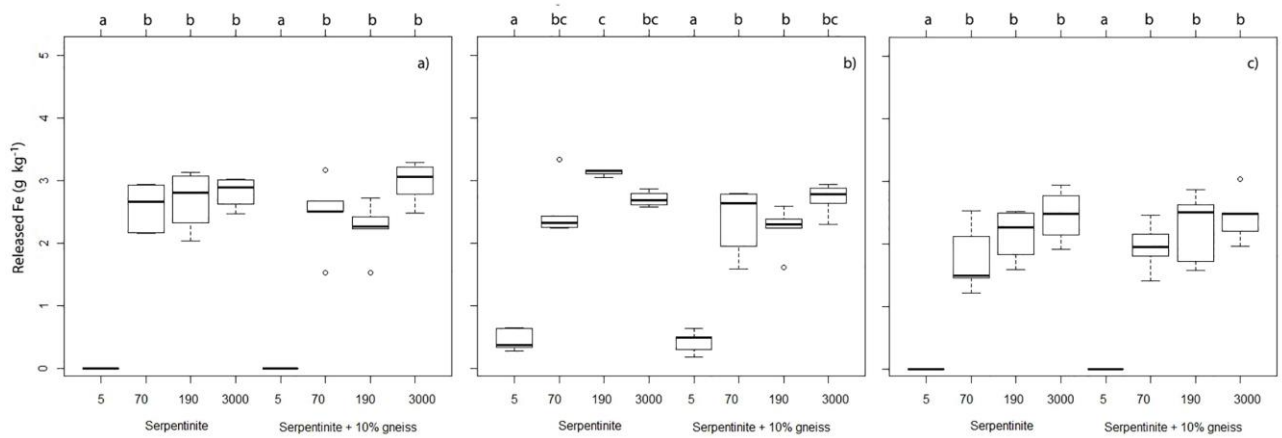

Fig.5 Iron released from the *Gt-sand* (a), *Pi-Gt-sand* (b) and *InsP6-Gt-sand* (c) systems positioned between the organic and surface mineral soil horizons along the serpentinite chronosequence (S5, S70, S190 and S3000) and the serpentinite + 10% gneiss chronosequence (SG5, SG70, SG190 and SG3000). The letters above the boxes evidence significant differences.